Spatiotemporal Chaos in The Regime of the Conserved Zakharov Equations

X. T. He[1,2] and C. Y. Zheng[2]

[1]*Chinese Center of Advanced Science and Technology (World Laboratory), P.O. Box 8730, Beijing 100080, People's Republic of China*

[2]*Center for Nonlinear Studies and Laboratory of Computational Physics, Institute of Applied Physics and Computational Mathematics, P.O. Box 8009, Beijing 100088, People's Republic of China**

(Received 26 August 1993)

It is first shown from the modulation instability of the conserved Zakharov equations that regular soliton patterns with a periodic sequence in space and time, and spatiotemporal chaos with irregular localized patterns, are formed in the different regions of the unstable wave numbers. The route from quasiperiodic to the coexistence of quasiperiodic and subharmonic, then from quasiperiodic and subharmonic to subharmonic, and furthermore to spatiotemporal chaos evolving from regular spatial patterns, is found. The formation mechanism of irregularly localized patterns is also revealed.

PACS numbers: 47.10.+g, 52.35.Mw

Spatiotemporal chaos in a continuum Hamiltonian system is an important subject used to investigate the long-term behavior of a volume preserving system with an infinite number of degrees of freedom, which leads to the soliton pattern structure. To our knowledge, so far, little work has been done on this problem in plasmas.

In the present Letter, we investigate the pattern dynamics and the feature of spatiotemporal chaos evolving from spatial patterns first using the conserved one-dimensional Zakharov equations (ZE's) [1],

$$\begin{aligned} i\partial_t E + \partial_x^2 E &= nE, \\ \partial_t^2 n - \partial_x^2 n &= \partial_x^2 |E|^2. \end{aligned} \tag{1}$$

Here $E(x,t)$ is a slowly varying envelope of the electric field, and $n(x,t)$ is an ion-acoustic density.

So far the ZE's are the most extensively studied model used to describe strong turbulence in plasmas. This system has three conserved quantities, i.e., the quasiparticle number, the momentum, and the total energy of the system.

The linearized stability analysis of the perturbation $\exp[i(k'x - \omega t)]$ from a spatially homogeneous field E_0 for Eqs. (1) gives the growth rate of the modulational instability (MI) as [2]

$$\gamma = \frac{k'}{\sqrt{2}}\left\{[(1 - k'^2)^2 + 8E_0^2]^{1/2} - (1 + k'^2)\right\}^{1/2}, \tag{2}$$

for $0 < k' < \sqrt{2}E_0$.

It was realized the localized patterns are formed from MI, and the single soliton for such Hamiltonian systems has analytically been obtained [1].

Equations (1) are a near-integrable system [2] and have at least two kinds of fixed points: a center at (0,0) and a saddle at $(E_0, 0)$. In a simple case wherein only one specified unstable wave number k', which satisfies Eq. (2), is considered, we solve the linearized Eqs. [1] in initial values $(E_0, 0)$ and obtain the eigenvalues

$$\lambda_1 = \left\{\tfrac{1}{2}k'^2[(1 - k'^2)^2 + 8E_0^2]^{1/2} - (k'^2 + 1)\right\}^{1/2} \equiv \lambda_0,$$

$$\lambda_2 = -\lambda_0,$$

$$\lambda_3 = i\left\{\tfrac{1}{2}k'^2[(1 - k'^2)^2 + 8E_0^2]^{1/2} + (k'^2 + 1)\right\}^{1/2} \equiv i\omega_0,$$

$$\lambda_4 = -i\omega_0,$$

and the eigenfunctions $f = \sum_{i=1}^{4} c_i e^{\lambda_i} f_i$, where $f_i = (k'^2, \lambda_i, -g_i, -\lambda_i g_i)$, c_i is coefficient, and $g_i = k'^2 + \lambda_i/E_0$. Obviously the saddle is in (f_1, f_2) subspace.

We now discuss numerical simulations of Eqs. (1) to investigate the global behavior and choose the initial condition to adjoin the saddle, which at $t = 0$ a very small spatial inhomogeneity is added on the spatial homogeneous state, $\Psi_0 = (E_0, 0, 0, 0)$, as follows [2]:

$$\Psi = \Psi_0 + (c_1 f_1 + c_2 f_2) E_0 \cos(k'x)/500, \tag{3}$$

where $\Psi_0 = (\mathrm{Re}E, \mathrm{Im}E, n, \partial_t n)_{t=0} = (E_0, 0, 0, 0)$, and factor $\frac{1}{500}$ is only to show that this is a very small perturbation adjusted for convenient calculations. Our initial condition ensures that the trajectories in phase space will locally lie in a saddle subspace. The case $c_1 = c_2 = 1$, which corresponds to the most stable orbit far from the homoclinic (HMO) [2], has been chosen in the discussion below.

The split-step method for E with a preestimate for density perturbation n is first used to compute Eqs. (1) with the periodic boundary condition in which the spatial grid L is chosen, so that $k'L = 2\pi$, and the number of grids is 64. During the computation the conserved quantities are preserved to the order of 10^{-6}.

It is noticed from the numerical results that by varying with $k = k'/\sqrt{2}E_0$, one finds a bifurcation point at $k_c \leq 0.9295$, which divides the system into completely different dynamic behaviors both temporally and spatially.

For $k_c < k \leq 1$, the long-term behavior of manifolds in phase space is only a single loop starting from and returning to the same saddle $(E_0, 0)$ to form the Kol'mogorov-Arnol'd-Moser torus as seen in Fig. 1(a). The envelope amplitude of the electric field is performing an exactly periodic oscillation [Fig. 1(b)]. Simultaneously, the power spectrum, as seen in Fig. 1(c), is of an isolated discrete distribution with equal frequency interval, which shows a sharp peak for $k = 0.98$ at the fundamental frequency

 0031-9007/95/74(1)/78(4)$06.00

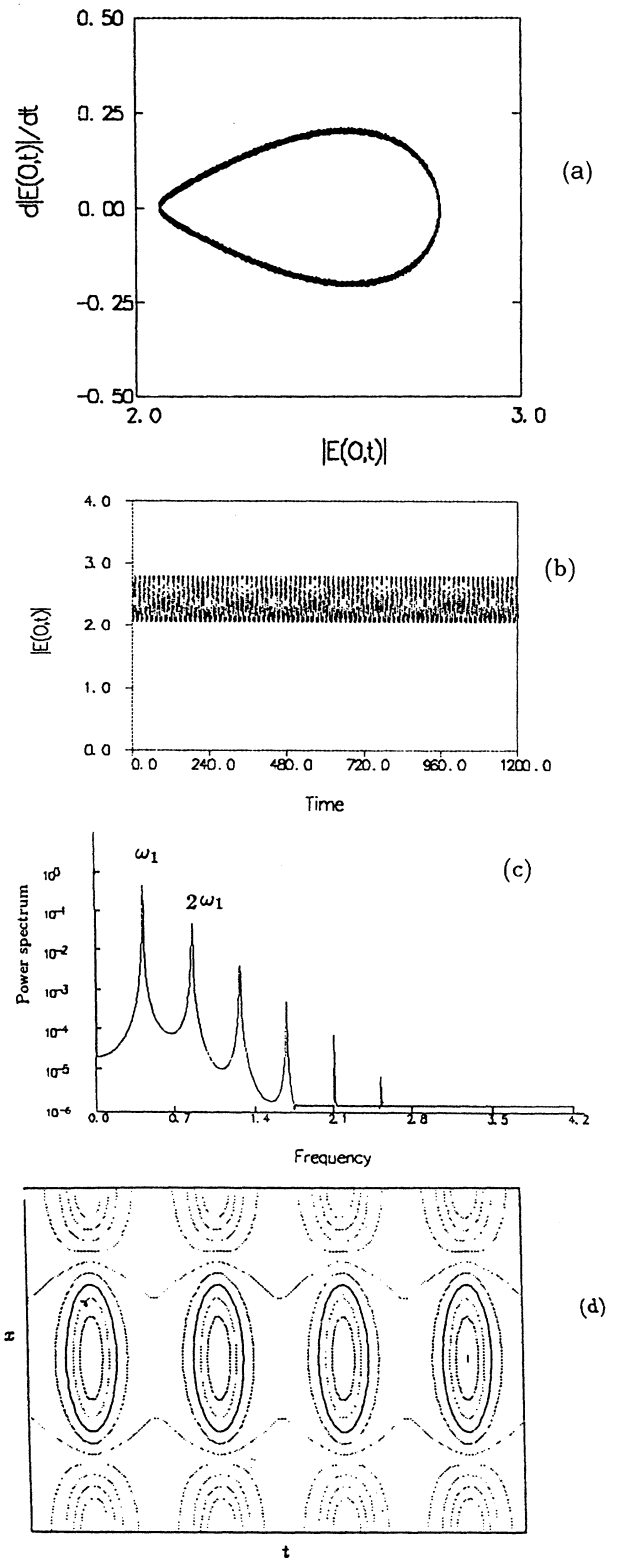

FIG. 1. Manifolds of phase space from the saddle point $(E_0, 0)$ at $x = 0$ for $k = 0.98$, (b) envelope amplitude $|E(x,t)|$ versus time for $k = 0.98$, (c) power spectrum for $k = 0.98$, and (d) contours of $|E(x,t)| = \text{const}$ for $k = 0.98$, $t = 500-550$.

$\omega_1 = 0.4188$ and is excited from the spatially homogeneous state and nth ($n = 2, 3, 4, \ldots$) harmonics of ω_1. However, the intensities of the harmonic spikes are extremely weak compared with the fundamental one. These features show that there exists an exactly periodic recurrence, like the Fermi-Past-Ulam (FPU) [3] process. For the spatial characteristics, we see from Fig. 1(d) that regularly localized patterns with a spatially and temporally periodic sequence are formed in the evolution of this system. These solutions propagate undisturbed with a constant speed. We observed that each one of these solutions is of symmetry and rapidly exponential decay in two sides around peak amplitude and is similar to single soliton solution of Eqs. (1) in the form $E(x,t) \sim \operatorname{sech}\alpha\xi$, where α^{-1} is the half-width and $\xi = x - ut$, u is a constant speed [1]. Thus, the ZE's system for $k_c < k < 1$, indeed, is executing a regular motion with coherent patterns. When k is reduced to 0.93, the motion in a two-cycle [Fig. 2(a)], which corresponds to localized patterns with slightly different structures [Fig. 2(b)], emerges, and the pseudorecurrence appears.

When $k < k_c$, the evolution of trajectories in phase space with the long lapse of time exhibits clearly irregular homoclinic orbit crossings filling up substantial portraits of phase space as shown in Fig. 3(a). At the same time,

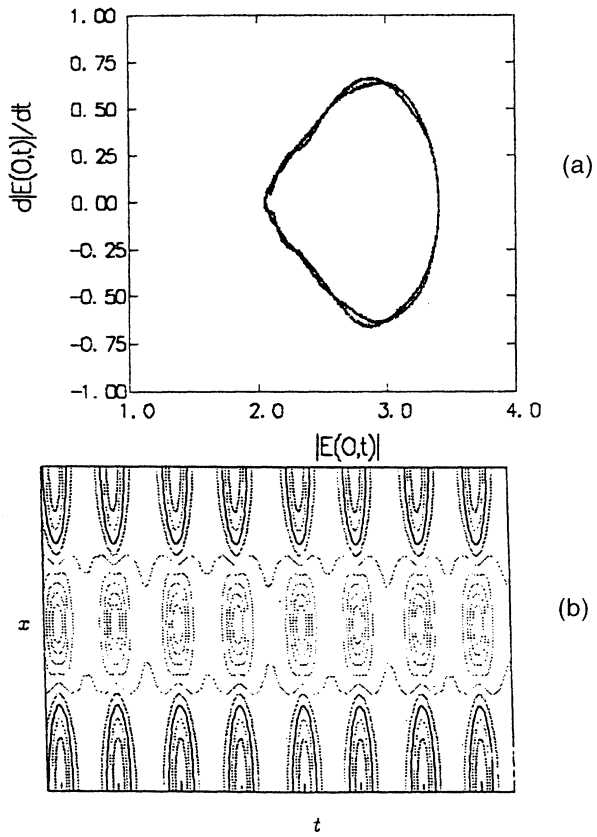

FIG. 2. Manifolds of phase space for $k = 0.93$, and (b) contours of $|E(x,t)| = \text{const}$ for $k = 0.93$, $t = 350-425$.

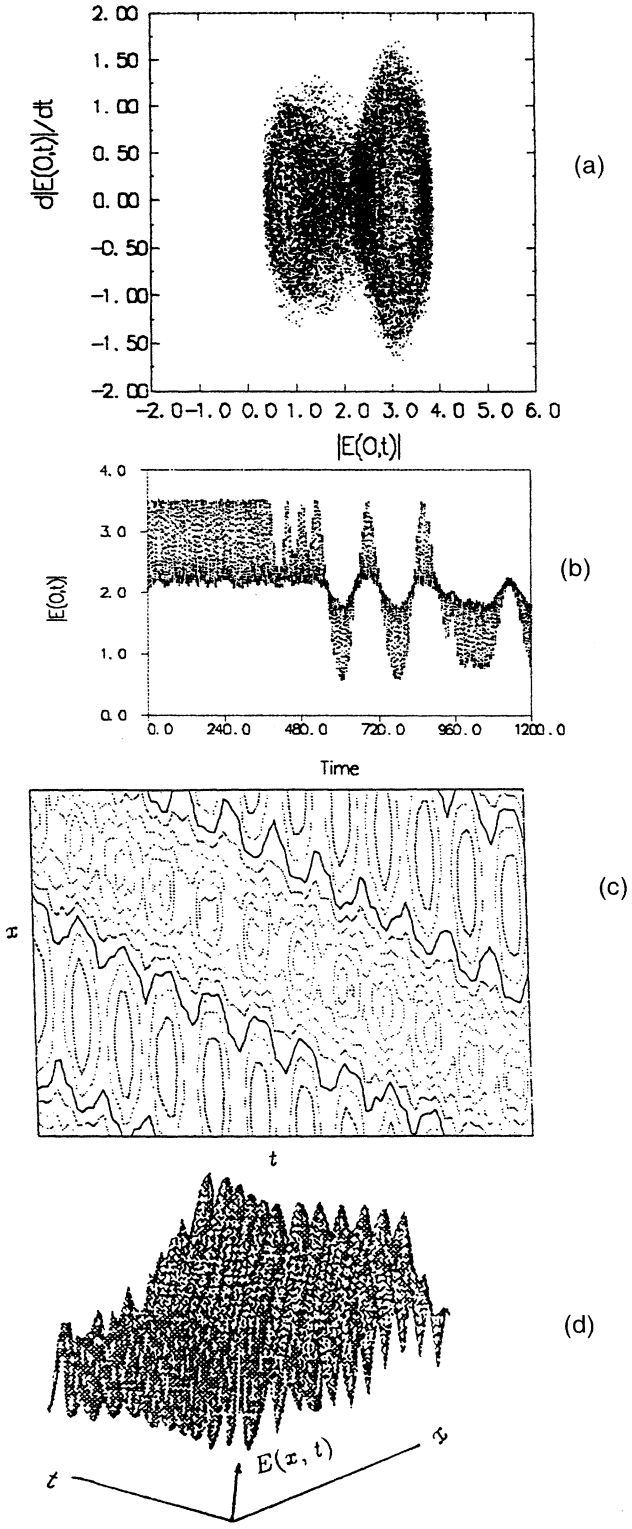

FIG. 3. The long-term behavior of $|E(x,t)|$ for $k = 0.88$. (a) Manifolds of phase space at $x = 0$, (b) envelope amplitude $|E(x = 0, t)|$ versus time, (c) contours of $|E(x,t)| = \text{const}$, $t = 500-550$, and (d) spatially localized structure, $t = 500-550$.

amplitude of the electric field experiences a quasiperiodic oscillation and exhibits stochastic behavior as seen in Fig. 3(b). That the contours for $E(x,t) = \text{const}$ in Fig. 3(c) are distorted indicates the existence of many irregularly localized patterns, which are still kept in the propagating process with stochastic speeds as shown in Fig. 3(d). The above feature illustrates the evolution of the spatial pattern that follows the temporal chaos.

Furthermore, the largest Lyapunov exponent with the definition

$$L_e = \lim_{t\to\infty} \lim_{D(t=0)\to 0} \left\{ t^{-1} \ln \left[\frac{D(t)}{D(t=0)} \right] \right\}$$

is positive for $k < k_c$, as seen in Fig. 4, where $D(t) = |E_1(0,t) - E_2(0,t)|$, $E_1(0,t)$, and $E_2(0,t)$ denote the $E(x,t)$ from two neighboring points in phase space at $x = 0$. Thus, the temporal chaos associated with the spatial patterns for the continuum Hamiltonian system is clearly observed.

In order to understand the evolutive route to spatiotemporal chaos, we observe the structure of the power spectrum. When $k = 0.95$, ω_1 increases to 0.5732, and an incommensurate frequency component $\omega_2 = 0.1157$ and the linear combination $\omega_1 \pm \omega_2$ appear simultaneously in Fig. 5(a). When k is reduced to 0.93, in addition to $\omega_1 = 0.6471$, $\omega_2 = 0.2324$, and $\omega_1 \pm \omega_2$, where their spikes of spectrum are weakened, the subharmonics $(2n - 1)\omega_1/2$, $n = 1, 2, 3, \ldots$, appear in Fig. 5(b). When $k = 0.9295$, the quasiperiodic behavior disappears, and only subharmonics exist with the further enhanced spikes, as seen in Fig. 5(c). Furthermore, to reduce k, the power spectrum with a broad-band noiselike structure occurs in Fig. 5(d). Thus, the evolution from quasiperiodic to quasiperiodic and subharmonic, then from quasiperiodic and subharmonic to subharmonic, furthermore, to chaos is found in our system. For the different c_1 and c_2, the above route is also observed.

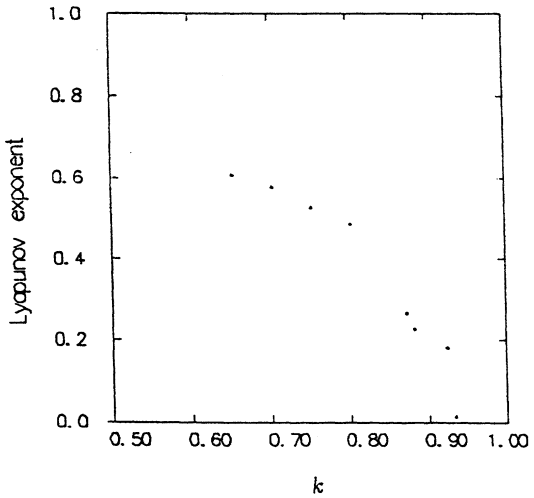

FIG. 4. Lapunov exponent versus k.

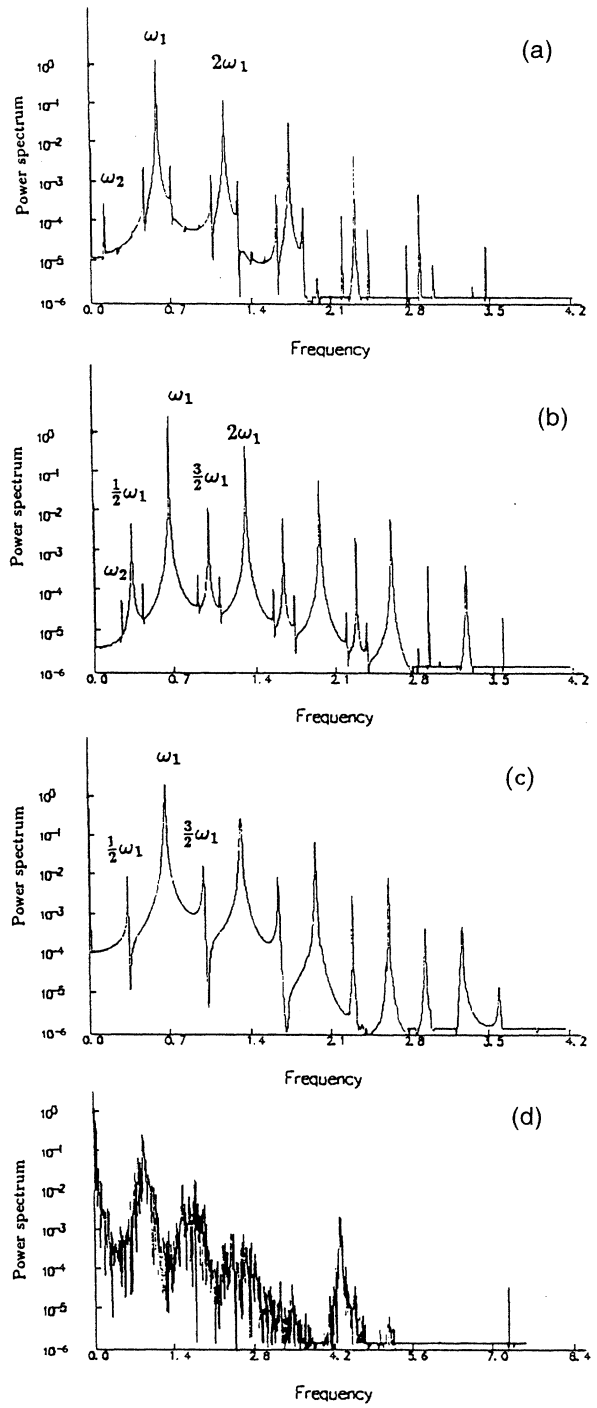

FIG. 5. Power spectrum. (a) $k = 0.95$, (b) $k = 0.93$, (c) $k = 0.9295$, (d) $k = 0.92$.

We will explain the reason in terms of the conception of harmonic oscillators by regarding each frequency as an oscillator. When k is 0.98, as seen in Fig. 1(c), the discrete spikes are isolated. However, when k approaches to k_c, the growth rate does increase, and ω_2, $\omega_1 \pm \omega_2$ and subharmonics make frequency intervals become narrow [see Figs. 5(a)–5(c)] and eventually oscillator overlapping for $k < k_c$ occurs because of the enhanced nonlinear interaction of the Langmuir wave with the ion-acoustic wave.

In order to further investigate the chaotic property of this system, we also computed the autocorrelation function [4] and found that the rapid decay of the correlator and the large Lyapunov exponents (Fig. 4) represent a very strong chaotic property for system, Eqs. (1). These justify the nature of the mixing of trajectories in phase space. Thus, there exists a Kol'mogorov-Sinai entropy [5].

To comprehend the formation of the irregular spatial structure, we investigate the energy shared by each of Fourier modes for $E(x,t) = \sum_n E_n(t)e^{ik_n x}$, where $k_n = 2\pi n/L$, $E_n = E_{k_n}$, and E_n versus time. This is similar to that in Ref. [6]. The spatially localized structure, indeed, can be described only in terms of finite modes. In our simulations, only eleven modes, i.e., $n = 5$, are included within the accuracy of 10^{-6} for conserved quantities, because the intensities of the higher Fourier modes have rapidly decreased. Energy initially confined to the master mode ($n = 1$), whose intensity increases with k decreasing and is excited from the spatially homogeneous state by MI, would extend to high harmonic slave modes. These modes are periodic in the sense of the Fermi-Pasta-Ulam (FPU)-like recurrence for $k_c < k$ but are unstable and stochastic for $k < k_c$. In the latter case, the interaction of slave modes with the master one causes the latter to be unstable due to the reaction of slave modes, and transferring more and more energy from the master to high harmonics at a fast rate. Thus, the FPU-like recurrence breaks. It leads to the formation of spatially irregular patterns, which are influencing temporal chaos.

In summary, the dynamics of regular spatial patterns with a periodic sequence in time and space are shown, The route from the quasiperiod route to subharmonics to spatiotemporal chaos for Eqs. (1) is first found. Features of spatiotemporal chaos with the coexistence of temporal chaos and spatially irregular patterns are observed.

We would like to acknowledge the helpful discussions of Professor S. G. Chen, Dr. W. M. Yang, and Dr. Y. Tan. This work is supported by National Natural Science Foundation of China (NNSFC) under Grant No. 19175039 and Nonlinear Science Foundation of China.

*Mailing address.

[1] V. E. Zakharov, Zh. Eksp. Teor. Fiz. **62**, 1745 (1972).
[2] Y. Tan, X. T. He, S. G. Chen, and Y. Yang, Phys. Rev. A **45**, 6109 (1992).
[3] R. Fermi, J. Pasta, and S. Ulam, *Collected Papers of Enrico Fermi* (Chicago University Press, Chicago, 1955), p. 978.
[4] G. M. Zaslavsky, *Chaos in Dynamic Systems* (Harwood, London, 1985).
[5] B. V. Chirikov, Phys. Rep. **52**, 265 (1979).
[6] X. T. He and C. T. Zhou, J. Phys. A **26**, 4123 (1993).